JOURNAL OF CATALYSIS **108**, 263–267 (1987)

Activation of Amorphous Cu–Zr Alloys

Several studies have been carried out in the field of CO hydrogenation over amorphous alloys containing zirconium (*1–5*). In these reports, amorphous alloys were oxidized under reaction conditions and yielded high-surface-area catalysts. The oxidized amorphous alloys showed higher activities or selectivities than those of the oxidized crystalline alloys. Further, there were several reports about the catalytic properties over the intermetallic compounds between a transition metal and a lanthanide or actinide element (*6–9*). After treatment with oxygen or *in situ* oxidation these intermetallic compounds changed into lanthanide or actinide oxides and transition metals, and then they were active in hydrogenation. The oxidation of alloys provides a new way of preparing supported catalysts.

In our previous paper (*4*), we described the process of activation of Cu–Zr amorphous alloys from the results of a high-pressure DTA in various gas atmospheres and X-ray diffraction, as follows.

(1) The amorphous Cu–Zr phase swells due to the absorption of hydrogen, and then cracks are formed in the surface ZrO_2 layer. CO and H_2 penetrate into these cracks, and the methanation reaction take place in the amorphous Cu–Zr phase.

(2) Zirconium is oxidized by water or oxygen produced during the methanation.

(3) Zirconium content in the amorphous phase decreases due to the oxidation of zirconium. This makes the amorphous phase unstable and the alloy changes to crystalline Cu and ZrO_2. At the same time, new cracks may form in the newly formed ZrO_2 layer beneath the original ZrO_2 layer.

(4) This process produces a catalyst with a large surface area which contains fine Cu particles dispersed in ZrO_2.

In this paper, we carried out CO hydrogenation over several samples containing zirconium and estimated the oxidation and the increase in the surface area of an amorphous Cu–Zr alloy during the activation process as a function of duration time under various atmospheres. Then we found that the presence of water drastically promoted the oxidation and the increase in the surface area of an amorphous Cu–Zr alloy. The *in situ* oxidation and oxidation with water of amorphous alloys containing zirconium make active catalysts from amorphous alloys. The oxidation of amorphous alloys provides a new way of preparing supported catalysts.

Master alloys were prepared by arc-melting zirconium (99.6%) and a pure transition metal (>99.99% Cu and >99.99% Pd) together in an argon atmosphere. The master alloys were pulverized to produce 1- to 2-mm grains. From these master alloys, amorphous alloy ribbons of 0.01–0.03 mm thick and 0.5–1.5 mm wide were fabricated by a single-roll type melt-quenching method in an argon atmosphere. Sample D was obtained from sample A by annealing at 873 K for 30 min under vacuum. These alloy ribbons were cut into 2 mm length.

Samples F and H were prepared by coprecipitation of aqueous solutions of zirconium oxichloride and copper nitrate or palladium chloride with an aqueous solution of sodium carbonate. The precipitate was aged at 353 K for 2 h, followed by a thorough washing with distilled water, dried at 393 K for 5 h, and calcined at 673 K for 2 h in air. The powder was pelletized

0021-9517/87 $3.00

TABLE 1

Preparation Methods of Samples, Their Crystalline Phases, and BET Surface Areas

Samples	M/Zr (atomic ratio)	Preparation	Crystalline phase	Surface area (m^2/g)
A	70/30 (M = Cu)	Melt-quenching[a]	Amorphous	<1
B	60/40 (M = Cu)	Melt-quenching[a]	Amorphous	<1
C	33/67 (M = Cu)	Melt-quenching[a]	Amorphous	<1
D	70/30 (M = Cu)	Annealing[b]	Cu–Zr[c]	<1
E	70/30 (M = Cu)	Arc-melting[d]	Cu–Zr[c]	<1
F	70/30 (M = Cu)	Coprecipitation[e]	Cu_2O, CuO, Amorphous	50
G	25/75 (M = Pd)	Melt-quenching[a]	Amorphous	<1
H	25/75 (M = Pd)	Coprecipitation[e]	ZrO_2	52

[a] Described in the experimental section.

[b] Described in the experimental section.

[c] It could not be identified but perhaps it is a mixture of Cu–Zr metallic compounds.

[d] Described in the experimental section.

[e] Described in the experimental section.

with graphite. Then the pellets were pulverized to produce 0.5- to 1.5-mm grains. Table 1 summarizes sample results to estimate their crystalline phases and BET surface area.

One-half gram of the sample was put into a reactor tube of stainless steel. The temperature of the sample was measured by a thermocouple which was inserted in the center of the sample layer. For samples F and H, the reduction of samples was carried out before the reaction, passing pure hydrogen through the reactor at 523 K at a flow rate of 2.0 liters h^{-1} and 0.1 MPa for 5 h. The reaction was carried out at a total gas pressure of 6.0 MPa. The gas mixture of CO, H_2, and Ar ($CO/H_2/Ar = 31/64/5$, $O_2 <$ 1 ppm) in a cylinder was used without further purification. The products were passed through a tube maintained at 473 K, without being condensed at the outlet of the reactor, and introduced into GC analyzers, one equipped with a TCD and a column packed with active carbon (Gasukuro Kogyo, Inc.) to determine Ar, CO, CO_2, and CH_4, and another equipped with a FID and a column packed with Porapak-Q (Waters Associates, Inc.) to determine hydrocarbons and oxygenated compounds.

For activation of sample A, $\frac{1}{2}$ g of sample A was put into the reactor. Gases used here were hydrogen (>99.99%), nitrogen (>99.99%), and the gas mixture of CO and H_2 ($CO/H_2 = \frac{1}{2}$). The activation by water was carried out in the nitrogen stream saturated with water at 303 K. The treatment conditions employed were total flow rate, 2.0 liters/h^{-1}; total gas pressure, 0.1 MPa; and temperature, 500 K.

The crystalline phases in the sample were identified by X-ray diffraction. The average size of sample crystallites was estimated from the half-value width of X-ray diffraction peaks.

Surface analyses of the samples were carried out using an XPS (ESCAPAK 750, Shimazu) with Mg$K\alpha$ X-ray radiation. Surface sputtering by Ar^+ ion bombardment was carried out at 2 keV, 15 mA.

Table 2 shows the results of CO hydrogenation over various samples containing zirconium after the stationary conditions were obtained. The activities of samples A, B, C, D, E, and G reached a steady state after

TABLE 2

Results of the CO Hydrogenation at 6.0 MPa ($CO/H_2/Ar$ = 31/64/5) and the Flow Rate of 2.1 Liters h^{-1} in the Stationary State and the Surface Area after the Reaction

Samples	Temperature (K)	Conversion (% CO base)						S.A.[a] (m^2/g)
		CH_3OH	DME[b]	CH_4	CO_2	Others[c]	Total	
A	500	8.4	0.3	0.2	0.0	0.0	8.9	67
B	495	7.6	0.4	0.1	0.0	0.0	8.1	33
C	521	6.8	0.7	1.2	1.1	0.0	9.8	12
D	505	4.4	0.1	0.1	0.0	0.0	4.6	
	553	6.1	0.8	0.7	0.6	0.0	8.2	34
E	544	7.6	2.0	0.8	0.7	0.0	11.1	32
F	500	3.3	0.1	0.2	0.3	0.0	3.9	
	521	4.4	0.3	0.3	0.5	0.0	5.5	78
G	478	16.7	0.2	3.2	0.8	0.3	21.2	36
H	501	2.8	0.1	0.4	0.0	0.1	3.4	42

[a] Surface area, measured by BET method after the reaction.

[b] Dimethyl ether.

[c] Mainly C_2 heavier hydrocarbons and alcohols.

many hours of the induction period. After the reaction, the increases in the surface area were observed as shown in Table 2.

Over amorphous Cu–Zr alloys, especially those with low zirconium content (samples A and B), the main product was methanol. The selectivity to methanol over an amorphous alloy (sample A) was higher than that over samples D, E, and F prepared by methods other than the oxidation of an amorphous alloy with the same composition of sample A at the same conversion level. After the reaction, peaks from monoclinic ZrO_2, tetragonal ZrO_2, and metallic copper were observed in X-ray diffractographs of sample A as shown in Fig. 1.

Over sample G, methanol was mainly produced. Yokoyama *et al.* (*1*) reported that the similar catalyst prepared *in situ* from an amorphous $Pd_{35}Zr_{65}$ alloy was active in methanation under atmospheric pressure. It is known that a SiO_2-supported Pd catalyst was active in the methanol synthesis reaction even below atmospheric pressure. And our reaction conditions, which were at a lower temperature and a higher pressure than those employed by Yokoyama *et al.*, are favorable for producing methanol. The activity over a precipitated catalyst (sample H) was a relatively low level but the selectivities were the same as those over sample G.

Table 3 summarizes the crystalline

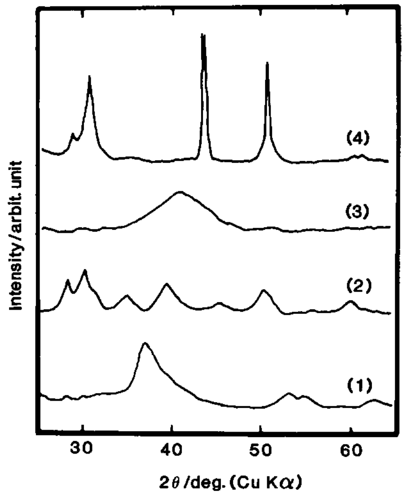

FIG. 1. X-ray diffractographs of samples before and after CO hydrogenation: (1) sample G before the reaction, (2) sample G after the reaction, (3) sample A before the reaction, (4) sample A after the reaction.

TABLE 3

Crystalline Phases and BET Surface Areas of Sample A after Treatment in Various Atmospheres

Atmosphere	Time (h)	Crystalline phase[a]	Surface area (m^2/g)
CO/H_2	24	Amorphous, Cu, ZrO_2(t)	<1
	50	Cu, ZrO_2(t), ZrO_2(m)	4
	96	Cu, ZrO_2(m), ZrO_2(t)	11
H_2O/N_2	1	Cu, ZrO_2(t), ZrO_2(m)	13
	24	Cu, ZrO_2(m), ZrO_2(t)	26
Air	5	Amorphous	<1
	74	Amorphous, Cu, ZrO_2(t)	<1
N_2	5	Amorphous	<1
	66	Amorphous	<1

Note. Temperature, 500 K; gas flow rate, 4.0 liters h^{-1} g^{-1}.
[a] ZrO_2(m), monoclinic zirconium oxide. ZrO_2(t), tetragonal zirconium oxide.

phases and surface areas of sample A after the activation. Figure 2 shows an increase in the BET surface area with time on stream after treatment of sample A with several atmospheres.

In the atmosphere in which oxidation of the sample did not occur, no increase in the surface area was observed. In N_2, little increase in the surface area and no oxidation were observed even after 66 h. In H_2, an amorphous phase changed into Cu and ZrH_2 and little increase in the surface area was observed.

In the atmosphere in which oxidation of the sample occurred, an amorphous phase changed into metallic copper and monoclinic zirconium oxide. In air, little increase in the surface area was observed after 72 h. In CO/H_2, a gradual increase in the surface area was observed. Then in H_2O/N_2, an increase in the surface area was observed even after 1 h.

A weak peak from (111) of tetragonal ZrO_2 was observed in the XRD of samples which had low surface areas. The peaks from (111) of monoclinic ZrO_2 were getting higher than those from (111) of tetragonal ZrO_2 with the increasing time of activation treatment, although this is not confirmed by quantitative analysis because of their poor crystallinities.

Figure 3 shows how the activities of CO hydrogenation over sample A after treatment with hydrogen and water change with time on stream at 500 K. The activity after treatment with hydrogen gradually increased as well as that without treatment. The treatment with water produces an active catalyst even in the initial stage. But under stationary conditions, the activities over the pretreated samples were relatively lower level than that over the *in situ* activated sample.

The surface states of sample A before and after the reaction were measured by

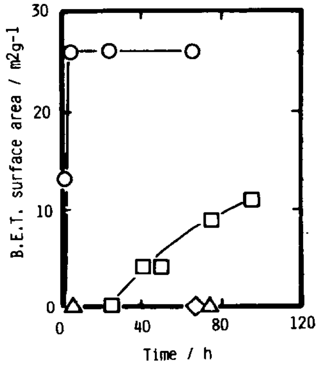

FIG. 2. Changes in the surface area during the treatment of a CZ7030A under 0.1 MPa of various atmospheres at 500 K. (◇) N_2, (△) air, (□) CO/H_2 = 0.5, (○) H_2O/N_2 = 0.04.

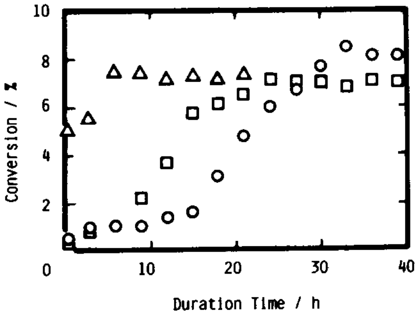

FIG. 3. Influence of the activation procedure on the catalytic activity of CZ7030A in CO hydrogenation. (○) No pretreatment, (□) pretreated with H_2 at 500 K for 1 h, (△) pretreated with H_2O and N_2 at 500 K for 1 h.

XPS. The ratio of peak areas (Cu 2*p*3/2/Zr 3*d*5/2) was 14.9 before the reaction and 1.8 after the reaction. This indicates that the migration of copper on the surface occurred during the oxidation of the sample. These condensations of copper were due to the phase separation of the amorphous phase into zirconium oxide and metallic copper. The Cu 2*p*3/2 spectrum and an Auger peak of copper showed the presence of Cu^+.

The results above and those previous (*4*) show that the presence of water drastically promotes the oxidation and the increase in the surface area. Two of the authors have already reported (*10*) that the oxidation of amorphous Au–Zr alloys occurred at room temperature and high humidity. It is known that Zr-based alloys begin to oxidize at an accelerated rate after initial protective oxidation (*11*). This breakaway phenomenon also occurs in water vapor. We consider that water vapor considerably accelerates crystalline growth for ZrO_2 in the surface oxide layer and facilitates the tetragonal-to-monoclinic phase transformation. Microcrack formation of the surface accompanies this phase formation. Sato and Shimada (*12*) have reported the same phenomenon in the surface oxide layer of yttrium-stabilized ZrO_2 (*12*). Water produced during the CO hydrogenation destroys the surface oxide layer and accelerates the oxidation of alloys. Then the oxidized alloys have large surface areas and show high catalytic activities.

REFERENCES

1. Yokoyama, A., Komiyama, H., Inoue, H., Masumoto, T., and Kimura, H., *Chem. Lett.*, 195 (1983).
2. Komiyama, H., and Inoue, H., *J. Fac. Eng. Univ. Tokyo Ser. A* **21,** 62 (1983).
3. Shimogaki, Y., Komiyama, H., Inoue, H., Masumoto, T., and Kimura, H., *Chem. Lett.*, 661 (1985).
4. Shibata, M., Ohbayashi, Y., Kawata, N., Masumoto, T., and Aoki, K., *J. Catal.* **96,** 296 (1985).
5. Shibata, M., Kawata, N., Masumoto, T., and Kimura, H., *Chem. Lett.*, 1605 (1985).
6. Coon, V. T., Takeshita, T., Wallace, W. E., and Craig, R. S., *J. Phys. Chem.* **80,** 1878 (1976).
7. Imamura, H., and Wallace, W. E., *J. Phys. Chem.* **84,** 3145 (1980).
8. Imamura, H., and Wallace, W. E., *J. Catal.* **65,** 127 (1980).
9. Daly, F. P., *J. Catal.* **89,** 131 (1984).
10. Kimura, H., Inoue, A., Masumoto, T., and Itabashi, S., *Sci. Rep. Res. Inst. Tohoku Univ., Ser. A* **33,** 183 (1986).
11. Kofstad, P., *in* "High-Temperature Oxidation of Metals," pp. 179–188. Wiley, New York, 1966.
12. Sato, T., and Shimada, M., *J. Amer. Ceram. Soc.* **68,** 365 (1985).

M. SHIBATA
N. KAWATA

Central Research Laboratories of
Idemitsu Kosan Company, Ltd.
Sodegaura, Kimitsu, Chiba 299-02, Japan

T. MASUMOTO
H. M. KIMURA

The Research Institute for Iron, Steel
and Other Metals
Tohoku University, Sendai 980, Japan

Received February 24, 1987; revised June 1, 1987